THE INFLUENCE OF THE ALVEOLAR RIDGE SHAPE ON THE STRESS DISTRIBUTION IN A FREE-END SADDLE REMOVABLE PARTIAL DENTURE SUPPORTED BY IMPLANT

Manoel M. Júnior[1], Rodolfo B. Anchieta[2], Eduardo P. Rocha[2], João A. Pereira[3],
Carlos M. Archangelo[1], Amilcar C. Freitas- Júnior[2], Erika O. Almeida[2]

[1] Instituto Federal do Parana-IFPR, Londrina, Brazil.

[2] Dental Materials and Prosthodontics Department, Faculty of Dentistry of Araçatuba,
São Paulo State University, São Paulo, Brazil.

[3] Department of Mechanical Engineering, Faculty of Engeneering of Ilha Solteira,
São Paulo State University, São Paulo, Brazil.

ABSTRACT

The alveolar ridge shape plays an important role in predicting the demand on the support tooth and alveolar bone in the removable partial denture (RPD) treatment. However, these data are unclear when the RPD is associated with implants. This study evaluated the influence of the alveolar ridge shape on the stress distribution of a free-end saddle RPD partially supported by implant using 2-dimensioanl finite element analysis (FEA).
Four mathematical models (M) of a mandibular hemiarch simulating various alveolar ridge shapes (1-distal desceding, 2-concave, 3-horizontal and 4-distal ascending) were built. Tooth 33 was placed as the abutment. Two RPDs, one supported by tooth and fibromucosa (MB) and other one supported by tooth

and implant (MC) were simulated. MA was the control (no RPD). The load (50N) were applied simultaneously on each cusp. Appropriate boundary conditions were assigned on the border of alveolar bone. Ansys 10.0 software was used to calculate the stress fields and the von Mises equivalent stress criteria (σ_{vM}) was applied to analyze the results.
The distal ascending shape showed the highest σ_{vM} for cortical and medullar bone. The alveolar ridge shape had little effect on changing the σ_{vM} based on the same prosthesis, mainly around the abutment tooth.

Key words: alveolar bone loss, endosseous dental implantation, finite element analysis, periodontal ligament.

INFLUÊNCIA DA FORMA DO REBORDO ALVEOLAR NA DISTRIBUIÇÃO DAS TENSÕES EM PRÓTESE PARCIAL REMOVÍVEL DE EXTREMIDADE LIVRE SUPORTADA POR IMPLANTE

RESUMO

A forma do rebordo alveolar representa um fator importante na previsão da demanda do suporte dentário e do osso alveolar em tratamentos com prótese parcial removível (PPR). Contudo, os dados não são claros quando uma PPR está associada com implantes.
Este estudo avaliou a influência da forma sagital do rebordo alveolar na distribuição das tensões de uma PPR de extremidade livre parcialmente suportada por implante usando a análise de elementos finitos (AEF) bidimensional.
Foram elaborados quatro modelos (M) matemáticos de um hemiarco mandibular simulando várias formas do rebordo alveolar (1-descendente distal, 2-côncavo, 3-horizontal e 4-ascendente distal). O dente 33 foi considerado como pilar. Duas PPRs, uma

suportada por dente e fibromucosa (MB) e outra suportada por dente e implante (MC) foram simuladas. MA foi o modelo controle (sem PPR). Uma carga (50N) foi aplicada simultaneamente em cada cúspide. Condições de contorno adequadas foram assumidas nas margens do osso alveolar. O software Ansys 10.0 foi usado para a análise das tensões segundo o critério das tensões equivalentes de von Mises (σ_{vM}) para a análise dos resultados.
A forma ascendente distal mostrou a maior σ_{vM} para osso cortical e medular. A forma do rebordo alveolar teve pouco efeito na alteração da σ_{vM} considerando o mesmo tipo de prótese, principalmente em torno do dente pilar.

Palavras chave: perda óssea alveolar, implante dentário endósseo, análise de elementos finitos, ligamento periodontal.

INTRODUCTION

The removable partial denture (RPD) has been associated with an osseointegrated implant to enhance stability and retention, which are harmed by the absence of dental support[1-3]. Thus, there are various combinations that use the implant as a support and/or retainer of the RPD base, mainly for free-end saddle clinical condition[3-17]. The presence of an implant on an edentulous distal edge, supporting the RDP acrylic resin base, allows a reduction

in the stress distributed on the alveolar ridge based on the conventional RPD biomechanics[18], overcoming some of the functional limitations of conventional dentures[1].

The alveolar ridge has a strong influence on the planning and biomechanics interpretation in an RPD treatment, mainly because of the viscoelastic difference of the dental support (1:13)[19], influenced by its anatomical shape in the saggital plane, affecting the stability and displacement of the RPD, and the distribution of the active forces through the support structures[20].

The alveolar ridge shape has been described based on 4 basic shapes in the saggital plane reference: concave, horizontal, distal ascending and distal descending. The literature showed that horizontal shaped edges have the best prognosis for dissipation of oblique forces on the alveolar ridge, increasing the success predictability of RPD treatment[20,21]. Although the descending distal, ascending distal and concave shapes are considered to have the worst prognosis because of the dissipation of oblique forces on the alveolar ridge, the data have not been evaluated through finite element analysis (FEA), which can help to analyze the events in the free-end saddle area and their influence on the abutment tooth from a new perspective.

This argument assumes relevance when the RPD is associated with an osseointegrated implant, because of the influence of the implant to support the acrylic resin base, reducing the stress on the support structures[6,18].

In addition, even when an implant is placed to support the RPD in the posterior region, the alveolar ridge shape can also influence the stress distribution on the alveolar ridge because based on its shape, the implant can adopt inclinations other than only perpendicular to horizontal plane[22].

A longitudinal study with RPD distally supported by osseointegrated implants showed adequate results after 4.5 years follow-up (2.5 mean time)[14]. However, there are no data regarding the influence of alveolar ridge shape on their results, as well as the angulations of the implants placed (parallel to the tooth or perpendicular to the crestal bone).

Consequently, there is a need to analyze the influence of the alveolar ridge shape when the RPD is associated with an osseointegrated implant. Thus, the purpose of the present study was to evaluate, through two-dimensional FEA (2-D FEA), the internal stress distribution by varying the alveolar ridge shape in the free-end saddle area during the association of the RPD with an osseointegrated implant.

MATERIAL AND METHODS

Four 2-D finite element models (M) of a mandibular hemiarch were built (AutoCAD 2006; Autodesk Inc., San Rafael, CA, USA) to simulate various alveolar ridge shapes in the saggital plane: 1) distal descending, 2) concave, 3) horizontal and 4) distal ascending (Table 1).

Each model showed the abutment tooth 33 in place and the absence of the teeth 34, 35, 36 and 37. The MA was used as control. A conventional RPD was simulated in the MB; and an osseointegrated implant was placed in the posterior region of the alveolar ridge to represent the MC. To consider the alveolar ridge

Table 1. Models (A, B and C) with the description of their components based on the alveolar ridge shape (1 – distal descending, 2 - concave, 3 - horizontal, and 4 – distal ascending)

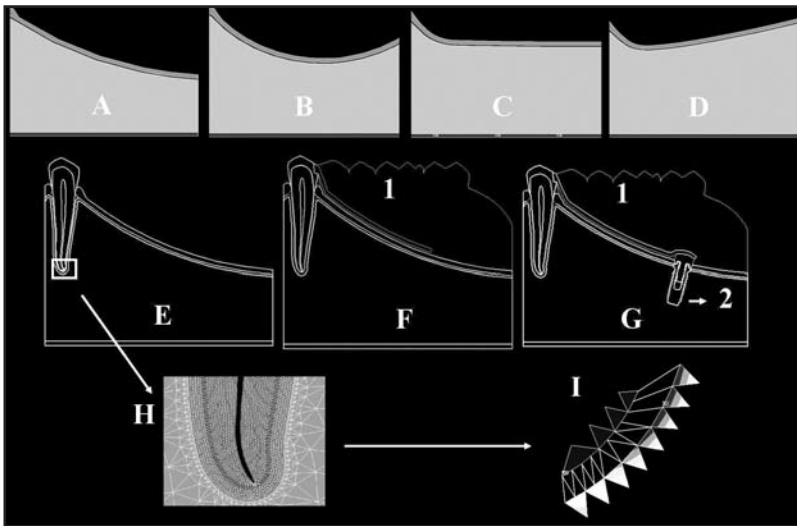| Models	Natural tooth	Artificial teeth	Osseointegrated implant	Alveolar ridge shape
A1		Absent	Absent	Distal descending
A2		Absent	Absent	Concave
A3		Absent	Absent	Horizontal
A4		Absent	Absent	Distal ascending
B1			3.75 x 10.00 mm	Distal descending
B2			3.75 x 10.00 mm	Concave
B3		34, 35, 36, 37	3.75 x 10.00 mm	Horizontal
B4			3.75 x 10.00 mm	Distal ascending
C1	33		3.75 x 10.00 mm	Distal descending
C2			3.75 x 10.00 mm	Concave
C3			3.75 x 10.00 mm	Horizontal
C4			3.75 x 10.00 mm	Distal ascending

Fig. 1: 1) Alveolar ridge shape description (A. distal descending; B. concave; C. horizontal; D. distal ascending). E. MA without RPD (1); F. MB with RPD (1); and G. MC with RPD (1) and implant (2). H. Mesh refinement at the apex root. I. beam3 elements used to represent the heterogeneous aspect of the PDL.
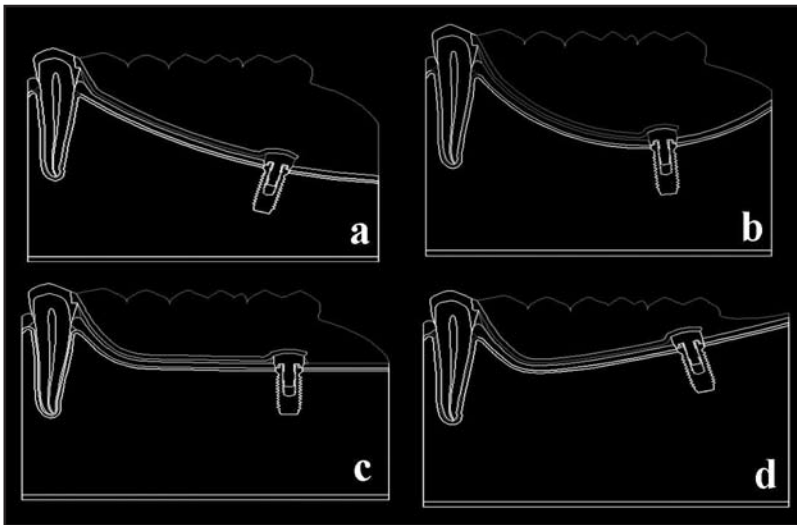

Fig. 2: Diagram showing the models C1(a), C2(b), C3(c) and C4(d) evidencing the implant inclination: clockwise direction (15°) in a; anti-clockwise direction (- 5°) in b; perpendicular to the oclusal plane (0°) in c; anti-clockwise direction (-15°) in d.

Table 2. Dimensions (mm) of the teeth 33 to 37.

Teeth	Ø Mesio - Distal	Height	Root length	Total Length
33	6.7	11.4	14	25.4
34	6.9	-	-	-
35	7.3	-	-	-
36	11.5	-	-	-
37	10.7	-	-	-

shape, each model followed the respective numbers above, such as MA1 which means a model with no RPD using a distal descending shape (Fig. 1).

The length and the shape of the alveolar ridge; the dimensions of the support and protective peri-odontal, with their biological distances (alveolar crest - cement/enamel junction - conjunctive insertion) were kept constant, in accordance with the specific literature[23].

The teeth dimensions were established by Sicher and Dubrul[24], and only the mesio-distal dimension of the artificial teeth 34, 35, 36 and 37 was considered, since they formed a single body with the acrylic resin base of the RPD with identical mechanical properties (Table 2).

A standard external hexagon implant (Nobel Biocare AB, Gothenburg, Switzerland) with dimensions of 3.75mm x 10 mm was used[4,6]. In all conditions, a healing abutment (Branemark System, RP 26560, Nobel Biocare, Gothenburg, Switzerland), with a length of 2mm, was used to support the RPD base. The implant assumed four inclinations in the saggital plane in accordance with the anatomical variation of the alveolar ridge shape for each model[22], namely (Figure 2): descending distal - 15° in the clockwise direction (+15°); concave - 5° in the anti-clockwise direction (- 5°); horizontal - perpendicular to the occlusal plane (0°); ascending distal - 15° in the anti-clockwise direction (-15°) (Fig. 2).

The FEA was performed in the program ANSYS 10.0 (Swanson Analysis Systems, Houston, PA, USA) from .sat extension Auto-CAD files. To generate the mesh, a 2-D solid element – plane 2 – was used. This is a triangular element defined by 6 nodes, with 2

degrees of freedom per node, and quadratic behavior for the displacement. This type of element is very suitable for modeling irregular meshes allowing an appropriate refinement of the mesh, mainly in the thin areas, such as the cortical bone, fibromucous, implant and periodontal ligament. The models showed nodes and elements ranging between 67.767 – 81.920; and 33.954 – 40.925, respectively.

The elastic parameters (Young's module and Poisson's coefficient) were used to consider the homogeneous, isotropic, and linearly elastic behavior for all structures, with exception of the periodontal ligament (PDL), which was considered as a heterogeneous structure (Table 3)[23-27].

The PDL was modeled using beam element (*Beam3*), which is a uniaxial element, defined by 2 nodes and 3 degrees of freedom per node. The disposition of the periodontal ligament fibers was established in accordance with the "in vivo" condition[21], based on the methodology proposed by Atmaram and Mohammed[25], with some modifications.

The use of the beam element demands the cross sectional area and the moment of inertia values. Grant et al.[30] established a fiber diameter dimension of 4 μm as suitable for representing the diameter of the periodontal fibers of a natural support tooth of an RPD. Thus, the values of the cross sectional area and the moment of inertia of each element were calculated using 4 μm as a reference value.

Consequently, the periodontal fibers can bear tensile and compression loads, similarly to those of Atmaram and Mohammed[25], and the bear flexural loads, an additional aspect used in the present study. Thus, the following formulas were used:

$A = \pi \cdot (r)^2$

$I = \pi \cdot (d)^4 / 64$, with: A = Cross sectional area; I = Moment of inertia; π = Value of 3.14; r = 2 x 10^{-6} m; d = 4 μm or 4 x 10^{-6} m.

The cross sectional area (A) and the moment of inertia (I) of each element were (in mm^2): **A = 1.256 x 10^{-5}** and **I = 0.785 x 10^{-12}**.

Four groups of periodontal fibers were represented in saggital plane with beam elements: crest-dental, horizontal, oblique and apical (Fig. 1). Once the beam element is related with nodes in each extremity, it was possible to use 412 beam elements, allowing an adequate refinement in accordance with the mesh generation of the cortical bone and dentin structures.

To simulate the mandibular symmetry, the entire right and left sides were fixed on the orthogonal axis x. The bottom of the model was fixed on the two x and y orthogonal axes (Fig. 3).

The distributed loading (50 N) was simultaneously performed on each cusp, in 5 points of 10N to prevent punctual occlusal contact[30] (Fig. 3).

The von Mises equivalent stress criteria (σ_{vM}) was used to establish the stress fields. Fibromucous, cortical and medullar bone were individualized. For more precise data, 4 areas were selected to perform the analysis in those structures (Fig. 3): 1) root apex; 2) distal bone crest; 3) anterior half of the alveolar ridge; 4) posterior half of the alveolar ridge.

Table 3. The mechanical properties of the materials and structures used in the study.

Structure	Young Module E (GPa)	Poisson's Coefficient	References
Enamel	41.0	0.30	24
Dentin	18.60	0.31	25
Periodontal Ligament	0.35	0.45	23
Fibromucous	0.68	0.45	24
Cortical Bone	13.70	0.30	25
Medullar Bone	1.37	0.30	25
Implant (Ti)	103.4	0.35	26
Healing abutment (Ti)	103.4	0.35	26
CoCr Structure	185	0.35	27
Acrylic Resin	8.30	0.28	24
Artificial Teeth	8.30	0.28	24

RESULTS
Cortical Bone
Table 4 shows the σ_{vM} in the areas 1, 2, 3 and 4 for the cortical bone.

The alveolar ridge shape showed different influences on the σ_{vM} distribution and intensity when the RPD was placed (MB). The most evident influence of the RPD was in the apex (area 1), with an increase of 400% in the σ_{vM} independently of the ridge shape.

The distal ascending and descending shapes showed the highest changes in the σ_{vM} at the distal crest bone (area 2) and alveolar ridge (areas 3 and 4). The horizontal and concave shapes showed little effect in the areas 2, 3 and 4.

The osseointegrated implant (MC) had no effect in the σ_{vM} at the areas 1, 2 and 3, independently of the alveolar ridge shape. The most evident change was in the area 4, closer to the implant neck, mainly for the distal ascending shape.
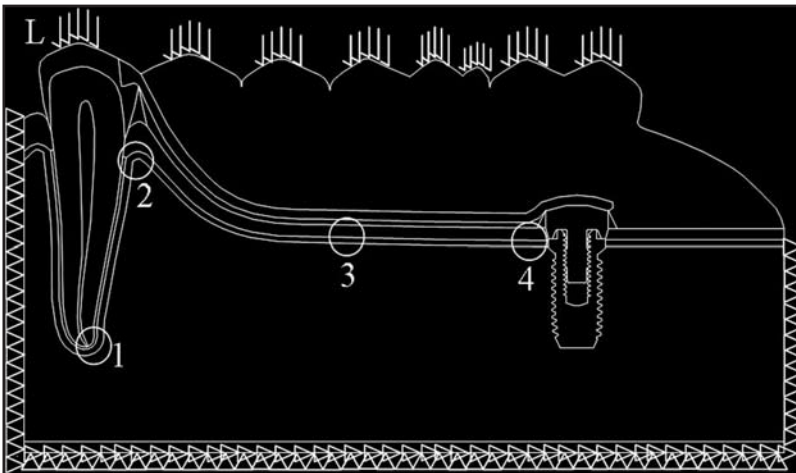
Medullar bone
Table 5 shows the σ_{vM} in the areas 1, 2, 3 and 4 for the medullar bone.

At the apex (area 1) of the MB, the σ_{vM} was higher (55-80%) than that observed in MA, with no alveolar ridge shape influence.

The distal descending shape had the highest influence in area 2 (distal crestal bone) for the MB.

The RPD had a strong influence in the σ_{vM} of the alveolar ridge (areas 3 and 4) increasing the stress up to 400%.

Similarly to that observed in the cortical bone, the σ_{vM} at the apex of the MC (osseointegrated implant) was lower (~20%) than that observed in MB; however there is no influence of the alveolar ridge shape.

Fig. 3: The entire right and left sides were fixed on the orthogonal axis x. The bottom of the model was fixed on the two orthogonal axes x and y. The distributed loading (L) was performed simultaneously on each cusp. Areas: 1 (apex), 2 (distal crestal bone), 3 (anterior half of the alveolar ridge), and 4 (posterior half of the alveolar ridge) selected for the analysis.

Table 4. von Mises stress (σvM), in MPa, for the specific areas of the cortical bone: 1) root apex; 2) distal bone crest; 3) anterior half of the alveolar ridge; 4) posterior half of the alveolar ridge.

Model	Area 1	Area 2	Area 3	Area 4
A1	8.61	76.31	16.97	16.97
A2	8.66	76.80	17.08	17.08
A3	8.97	97.14	17.68	17.68
A4	8.95	80.51	17.89	17.89
B1	34.31	92.78	17.60	17.60
B2	32.45	88.40	16.46	16.46
B3	35.21	87.17	26.55	17.89
B4	35.39	93.55	25.94	25.94
C1	33.36	90.06	17.16	17.16
C2	31.00	85.00	15.57	31.00
C3	33.69	91.72	25.41	33.69
C4	34.12	93.51	25.64	76.54

Table 5. von Mises stress (σvM), in MPa, for the specific areas of the medullar bone. 1) root apex; 2) distal bone crest; 3) anterior half of the alveolar ridge; 4) posterior half of the alveolar ridge.

Model	Area 1	Area 2	Area 3	Area 4
A1	11.30	7.57	1.98	1.98
A2	11.37	7.60	2.27	2.27
A3	11.34	7.58	2.61	2.61
A4	13.21	7.55	5.66	1.88
B1	17.42	13.19	8.96	8.96
B2	16.08	11.54	10.03	10.03
B3	17.70	11.76	11.76	8.79
B4	16.14	10.66	12.03	9.28
C1	13.97	10.65	9.00	4.03
C2	12.98	11.14	10.79	3.75
C3	13.38	11.76	11.76	3.64
C4	14.37	10.33	12.35	4.28

In the area 2, the implant did not change the σ_{vM} comparing with the equivalent area in the MC.

The distal ascending and descending shapes showed the highest influence on the alveolar ridge (areas 3 and 4) in the MC. However, in the anterior region (area 3), the σ_{vM} was similar to that observed in MB.

Fibromucosa

Table 6 shows the σ_{vM} in the areas 3 and 4 for the fibromucosa.

In area 3, the anterior half of the alveolar ridge of the MB and MC, the σ_{vM} was up to 70% higher than the equivalent area of the MA. The horizontal shape showed the highest σ_{vM} for both models.

The alveolar ridge shape had no influence on area 4 for either condition (models B and C); however, the σ_{vM} in the MC came back to that observed in the MA.

Table 6: von Mises stress (σvM), in MPa, for the specific areas of the fibromucosa. Area 3: anterior half of the alveolar ridge; Area 4: posterior half of the alveolar ridge.

Models	Area 3	Area 4
A1	8.12	8.12
A2	8.22	8.22
A3	8.17	8.17
A4	8.53	8.53
B1	9.17	9.17
B2	13.72	13.72
B3	14.04	14.04
B4	12.97	12.97
C1	13.89	7.20
C2	13.85	7.16
C3	14.18	7.20
C4	12.91	6.56

DISCUSSION

The development of 3-D finite element models compatible with oral reality is not an easy task, mainly to reproduce the behavior of the RPD and its correlation with the buccal structures. Because of the large number of anatomical structures present in the lower jaw, the development of reliable three-dimensional models for finite element analysis in this study requires the use of tomography images with excellent resolution.

This becomes a challenge for the recognition of bony, dental and soft tissues, due to the fact that obtaining the models requires the manipulation of CT images through a series of specific softwares, which begin by rebuilding the solids, generating the finite element mesh, and generating files compatible with the finite element program. Therefore, a 2-D study can generate good results if it is suitably conducted, as it allows a series of considerations and interpretations to be made that are much closer to the reality of the intra-buccal environment[21,22].

For example, the heterogeneous aspect of the PDL performed structurally and mechanically was closer to that observed under "in vivo" conditions, in agreement with reports by Atmaram and Mohammed[25] and Berkovitz et al.[23].

This enabled adequate conditions for discussing the influence of the alveolar ridge shape on the stress distribution by FEA. It is emphasized that the RPD text books are generally restricted to the biomechanical explanations based on the theoretical description of classical mechanics, without showing quantitative data regarding the influence of the alveolar ridge shape on the free-end saddle area[18]. In this context, the present study showed differences in the stress distribution pattern based on the different shapes, adding data to this subject, including the influence of osseointegrated implants.

At first, regarding the influence of the RPD on the support structures (MB), it was found that the RPD promoted higher stress around the abutment tooth for the cortical bone (areas 1 and 2); and on the alveolar ridge (areas 3 and 4) for the fibromucosa. For the cortical bone, the distal ascending shape showed the highest σ_{vM} in the alveolar ridge. For the fibromucosa, the horizontal shape showed the highest σ_{vM} in the areas 3 and 4.

The results partially reproduce what is established by the literature, which shows the distal descending shape as the most harmful in comparison with others shapes[18]. The highest influence of the distal descending shape was therefore only observed in the medullar bone (Table 5).

In general, the alterations in the σ_{vM} were more evident between models with the same alveolar ridge shape, than those based on the alveolar ridge shape influence only, mainly in areas 1 and 2 for both models (MB and MC). For some structures, such as the cortical bone of the MB, the difference of the σ_{vM} among the four alveolar ridge shapes was small. The benefits of the implant were more pronounced in area 4 of the fibromucosa, and in the areas 1 and 4 of the medullar bone. In those areas, the σ_{vM} was lower than that observed in the MB. However, the σ_{vM} was similar in the areas 1, 2 and 3 of the corti-

cal bone and fibromucosa comparing the MB with the MC, with no shape influence in either of them. One interesting aspect observed in the present study was for the models C2, C3 and C4, whose σ_{vM} on the left side of the implant increased by up to 290%. The result can be explained by the proximity of the implant to the loading area. Far from the loading area, the σ_{vM} was less pronounced.

Because of some similarities regarding σ_{vM} magnitude among different shapes, it cannot be emphatically stated that the differences observed in the models unrestrictedly justify that the distal descending shape is worse or more damaging to the integrity of the support structures. In fact, the distal ascending shape presented the highest σ_{vM} concentrations in the majority of the areas and aspects considered, followed by distal descending shape, but the σ_{vM} differences among four shapes were small for some conditions, such as area 1 of the MB. It was shown that the horizontal and concave shapes also promoted the highest alterations in σ_{vM} (Tables 5 and 6).

In connection to this, the study suggests that others aspects might be more relevant in RPD planning than the influence of alveolar ridge shape, such as: the qualitative and quantitative aspects of dental support, the antagonist arch, the root anatomy of the abutment tooth, the dental position and alignment, the integrity of the tooth crown, the tooth mobility and the bone loss, as well as the bone loss at the alveolar ridge. These factors associated with the fibromucous viscoelasticity, will determine how unstable the RPD can be, mainly in the face of horizontal and oblique demands.

It is, however, emphasized that the data were obtained through a 2-D FEA, with vertical loading only. It is possible to obtain different results under different load conditions, which would become necessary, in view of the data obtained in this study, and which were not predicted or evidenced by the specific literature or other methods[20].

Although the distal ascending shape showed the highest σ_{vM} followed by distal descending shape for cortical and medullar bone, the four different shapes of the alveolar ridge had little effect in the σ_{vM}.

CORRESPONDENCE
Dr. Rodolfo B Anchieta
Rua Jose Bonifacio, 1193
Vila Mendonça, 16015-050
E-mail: rodolfoanchieta2@hotmail.com

REFERENCES

1. Mericske-Stern R. Removable partial dentures. Int J Prosthodont 2009;22:508-511.

2. Armellini DB, Heydecke G, Witter DJ, Creugers NH. Effect of removable partial dentures on oral health-related quality of life in subjects with shortened dental arches: a 2-center cross-sectional study. Int J Prosthodont 2008;21:524-530.

3. Ganz SD. Combination natural tooth and implant – borne removable partial denture: a clinical report. J Prosthet Dent 1991;66:1-5.

4. Battistuzzi PG, Van Slooten H, Kayser AF. Management of an anterior defect with a removable partial denture supported by implants and residual teeth: a case report. Int J Oral Maxillofac Implants 1992;7:112-115.

5. George MA. Removable partial denture design assisted by osseointegrated implants. J Calif Dent Assoc 1992;20:64-66.

6. Keltjens HM, Kayser AF, Hertel R, Battistuzzi PG. Distal extension removable partial dentures supported by implants and residual teeth: considerations and case reports. Int J Oral Maxillofac Implants 1993;8:208-213.

7. Giffin KM. Solving the distal extension removable partial denture base movement dilemma: a clinical report. J Prosthet Dent 1996;76:347-349.

8. Jang Y, Emtiaz S, Tarnow DP. Single implant – supported crown used as an abutment for a removable cast partial denture: a case report. Implant Dent 1998;7:199-204.

9. Turkyilmaz I. Use of distal implants to support and increase retention of a removable partial denture: a case report. J Can Dent Assoc 2009;75:655-658.

10. Pellecchia M, Pellecchia R, Emtiaz S. Distal extension mandibular removable partial denture connected to an anterior fixed implant-supported prosthesis: a clinical report. J Prosthet Dent 2000;83:607-612.

11. Carvalho WR, Barboza EP, Caúla AL. Implant-retained removable prosthesis with ball attachments in partially edentulous maxilla. Implant Dent 2001;10:280-284.

12. Starr NL. The distal extension case: an alternative restorative design for implant prosthetics. Int J Periodontics Restorative Dent 2001;21:61-70.

13. Mcandrew R. Prosthodontic rehabilitation with a swing-lock removable partial denture and a single osseointegrated implant: a clinical report. J Prosthet Dent 2002;88:128-131.

14. Mitrani R, Brudvik JS, Phillips KM. Posterior implants for distal extension removable protheses: a retrospective study. Int J Periodontics Restorative Dent 2003;23:353-359.

15. Kuzmanovic DV, Payne AGT, Purton DG. Distal implants to modify the Kennedy classification of a removable partial denture. a clinical report. J Prosthet Dent 2004;92:8-11.

16. Mijiritsky E, Karas S. Removable partial denture desing involving teeth and implants as an alternative to unsuccessful fixed implant therapy: a case report. Implant Dent 2004;13:218-222.

17. Uludag B, Celik G. Fabrication of a maxillary implant-supported removable partial denture: a clinical report. J Prosthet Dent 2006;95:19-21.

18. Mijiritsky E. Implants in conjuction with removable partial denture: A literatura review. Implant Dent 2007;16:146-154.

19. Cordaro L, Ercoli C, Rossini C, Torsello F, Feng C. Retrospective evalution of complete arch fixed partial dentures connecting teeth and implant abutments in patients with normal and reduced periodontal support. J Prosthet Dent 2005;94:313-320.

20. McGivney GP, Carr AB. McCraken's removable partial prosthodontics.10th ed. St. Luis: Mosby, 2000.

21. Kawasaki T, Takayama Y, Yamada T, Notani K. Relationship between the stress distribuition and the shape of the alveolar residual ridge: tree-dimensional behavior of a lower complete denture. J Oral Rehabil 2001;28:950-957.

22. Watanabe F, Hata Y, Komatsu S, Ramos TC, Fukuda H. Finite element analysis of the influence of implant inclination, loading position, and load direction on stress distribution. Odontology 2003;91:31-36.

23. Berkovitz BKB, Moxham BJ, Newman HN. The periodontal ligament in health and disease. 2nd ed. London: Ed. Mosby-Wolfe; 1995.

24. Sicher H, Dubrul EL. Sicher's Oral anatomy/By E.Lloyd Brubrul. 8th ed. St. Louis: Ishiyaku Euroamerica; 1988.

25. Atmaram GH, Mohammed H. Estimation of physiologic stresses with a natural tooth considering fibrous PDL structure. J Dent Rest 1981;60:873-877.

26. Ko CC, Chu CS, Chung KH, et al. Effects of posts on dentin stress distribution in pulp less teeth. J Prosthet Dent 1992;68:421-427.

27. Farah JW, Craig RG, Meroueh KA. Finite element analysis of a mandibular model. J Oral Rehabil 1988;15:615-624.

28. Sertgoz A, Guvener S. Finite element analysis of the effect of cantilever and implant length on stress distribution in a implant-supported fixed prosthesis. J Prosthet Dent 1996;76:165-169.

29. Williams DF. Biocompatibity of clinical implant materials, Boca Raton: CRC Press 1981.

30. Grant DD, Stern IB, Listgarten MA. Periodontics. 6nd ed. St. Louis: Ed. Mosby; 1988.